



<http://www.diva-portal.org>

Postprint

This is the accepted version of a paper presented at *13th International Conference on Indoor Air Quality and Climate, July 7-12, 2014, Hong Kong*.

Citation for the original published paper:

Karimipannah, T., Larsson, U., Cehlin, M. (2014)

Investigation of flow pattern for a confluent-jets system on a workbench of an industrial space.

In: *Indoor Air 2014: 13th International Conference on Indoor Air Quality and Climate* (pp. 192-199).

N.B. When citing this work, cite the original published paper.

Permanent link to this version:

<http://urn.kb.se/resolve?urn=urn:nbn:se:hig:diva-17859>

INVESTIGATION OF FLOW PATTERN FOR A CONFLUENT-JETS SYSTEM ON A WORKBENCH OF AN INDUSTRIAL SPACE

Taghi KARIMIPANH*, Ulf LARSSON, and Mathias CEHLIN

Faculty of Engineering and Sustainable Development, Department of Building, Energy and Environmental Engineering, University of Gävle, Sweden

*Corresponding email: tkh@hig.se

Keywords: Workbench, Ventilation, Thermal comfort, Confluent Jets, CFD

SUMMARY

A new air supply terminal based on confluent jets was installed on a workbench, in vicinity of a CNC machine, of an industrial space. The flow pattern and temperature field was carried out by CFD calculations and infrared camera imaging technique. A main goal of this technique is to save energy therefore the jet should distribute the air where it is desired. This is possible because the confluent jets system uses the benefits of both mixing (high momentum for better spreading of the air jet) and displacement (cleaner air in occupied zone).

The results show that thermal comfort and air quality analysis relies on consistent facts and is in good agreements with the existed standards.

It was shown that the supply terminal is able to spread the fresh air to the needed work area. This is an advantage of the high momentum air distribution system used in this investigation.

INTRODUCTION

As in residential and office buildings, the industrial spaces require also good ventilation performance to guarantee a healthy environmental condition and a better productivity. In investigation of Seppänen et al (2006) has been shown that there is a strong relationship between ventilation rate and working performance.

Karimipannah et al (2007 and 2008) have tested the performance of this system against other ventilation strategies, both experimentally and numerically. Cho et al (2008) compared confluent jets system with displacement ventilation system. They derived an empirical equation for the decay of maximum velocity from jet centerline based on the measured velocities. They also showed that the wall confluent jets system produces a greater horizontal spread over the floor than displacement jet and they confirmed that the confluent jet system in most cases performed better than the other existed ventilation systems.

This paper focuses on simulations of temperature field and flow pattern of an industrial warehouse using a confluent jets air supply terminal for a single worker. The results were verified by the infrared camera images taken at different sections of workplace. The supply system is very likely as a personalized ventilation system, because of the airflow is distributed close to worker to avoid unnecessary ventilation of other part of the work place. This modern confluent jets ventilation system developed and tested by a Swedish ventilation company in close collaboration with our university; have the capacity for both cooling and heating of residential, offices and industrial ventilation applications.

The purpose was to examine the flow pattern from two newly mounted Confluent Jets supply air terminal using FLIR infrared camera and Computational Fluid Dynamics (CFD) for studying the flow pattern.

MODEL SET-UP

The system analyzed, as can be figured out from Figure 1, is a single worker, his workbench and the confluent jets blowing into the corner. Figure 1 (right) represents the confluent jets only (with any expanded metal). It should be noted that without adding the metal sheet, right figure below, the airflow may cause draught. As shown in figure 1 (left) the worker is exposed directly to the air jet flow, thus we use an expanded metal to avoid the draught problem. In case without expanded metal and empty room, figure 1 (right) we blow directly to the wall for damping the highly flow turbulence.



Figure 1. Confluent jets supply device blowing towards worker with expanded metal.

The target is to analyze the indoor climate and develop an approach to thermal comfort and air quality parameters. The results are compared with ISO 7730 in order to conclude whether the implemented ventilation system helps the company to follow this standard.

Here, a model with some simplifications sets up to make it feasible for CFD simulations. In first case, see figure 2 (right) a “single room” with dimensions of $5 \times 5 \times 5 \text{ m}^3$; consists of a confluent jets supply device will be regarded as the main calculation domain. But for the second case, see figure 2 (left) a “single room” with dimensions of $5 \times 5 \times 5 \text{ m}^3$; consists of a worker, workbench and confluent jets supply device will be regarded as new calculation domain.

In order to analyze how the flow pattern and temperature field, issued from a confluent supply device, the ANSYS Gambit (modelling and meshing) and Fluent (simulation) software are used. The supply diffuser has its exhaust directed against a column with 11 cm from the wall. The reason for the placement is to create a good working environment for the standing worker at the workbench. The devices were plugged and adjusted so that the diffuser with expanded metal sheet to the arm of the machine had 63 Pa pressure drop. The main pipe has a diameter of 15 cm, 136 open nozzles of 5.6 mm in diameter; 33 l / s air flow and 27.5 °C supply temperature for heating purposes as shown in Figure 2 (left).

In CFD calculations these 136 small holes will be transformed into an equivalent area in order to simplify modelling and computation. The confluent Jets device itself is designed by using the spacing approach as described in Awbi (2003).

Finally, the worker mannequin and workbench are included in the model built with Airpak, whilst the simulation takes place in Fluent (2013). Some ventilation parameters such as Air Change Rate (ACR), mean age of air and Predicted Percentage of Dissatisfied (PPD) among the others, will be carried on. Furthermore, mesh independency, y plus, residuals and mesh quality are confirmed as well, to verify the quality of models.

For these calculations we use the well-known Renormalization Group (RNG) $k-\epsilon$ turbulence model. This method is a sub-method of the standard $k-\epsilon$ model developed by Yakhot and Orszag of Princeton University, see Lam (1992). The effects of the small scale turbulence are represented “by means of random forcing function in the Navier-Stokes equation” and they are continuously deleted from the governing equations expressing their effect through larger scale motions and a modified viscosity. Enhanced Wall Treatment method for $K-\epsilon$ RNG turbulence model was chosen for all model run here, both the one coming from Gambit and the one coming from Ansys Airpak. This combination was chosen because many researchers recommend it and provides more accurate solutions for jet impinging to a surface (walls) and also for economic reasons.

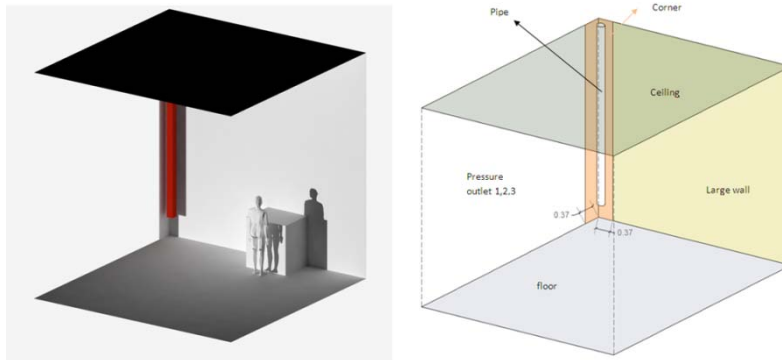


Figure 2. Model mock up for CFD simulations with worker and workbench (left) empty room (right).

In order to verify the mesh quality for the model; we used three runs for coarse grid, middle fine and fine grids. Meshes with hexahedral nodes which result in more accurate solutions than the others available are used, see André Bakker (2002).

The amount of cells, mesh density, has to be the adequate to capture the relevant flow parameters and the near wall zone mesh has to be accurate enough to deal with the boundary layer flow (y^+ , see “Wall treatment” under theory); in this zone quad and hex nodes are preferred than tetrahedral between others. Poor quality grid will cause imprecise solutions and probably slow convergence. The chosen mesh has 1,010,250 elements (every edge meshed at 0.02 m). The other three parameters, skewness, smoothness and aspect ratio have strongly influence the convergence and solution of the model.

Starting from the skewness, the picture taken from Gambit shows up that most of the nodes performing the mesh are in skewness “0” or top quality, although the worst element has a skewness value of 0.518005 what is almost 0.5 which was the maximum objective value.

Since there are no parameters to measure smoothness and aspect ratio quality, they were assessed while meshing.

Since temperature field is a key factor for thermal comfort, the energy model is going to be used in order to take into account and set temperatures of every element as well as to show how it is spread throughout the room.

It is worth mentioning that the images with FLIR infrared camera taken in workplace are used to properly define the temperature of every different part of the mock up.

Infrared thermography systems typically have accuracy specifications of $\pm 1.5^\circ$ or $\pm 2.0^\circ\text{C}$. Through proper camera handling, thermography images can provide quantitative surface temperatures on flat high emissivity materials ($\epsilon > 0.90$) with relatively high accuracy. It have been shown that the difference between instantaneously infrared thermography measurements individual thermocouples are within $\pm 0.6^\circ\text{C}$ for temperatures around $17\text{--}25^\circ\text{C}$ (Cehlin et al

2000). However, an analytical and experimental investigation performed with a high-emissivity solid screen placed in a typical airflow from a low-velocity diffuser in an office room show that the temperature of a solid screen can be around 1-2 °C warmer than the ambient air due to surrounding radiation (Cehlin et al 2002).

In order to provide and extract accurate values from the provided images, software called “ThermaCAM Researcher Professional 2.8” (see FLIR 2006) is used. The Temperatures obtained with this software are shown in table 1. The temperatures defined on table 1 were used as boundary conditions in addition to supplier velocity, equal to $9.85 \frac{m}{s}$ in a normal to boundary direction and assuming a density value $\rho = 1.225 \frac{kg}{m^3}$. The calculated effective area of the air supply terminal is equal to: $A = 3.3496 \cdot 10^{-3} m^2$ and the flow rate as $\dot{Q} = v A = 0.033 \frac{m^3}{s} = 33 \frac{l}{s}$

In the boundary conditions the turbulent kinetic energy of backflow air supply was reduced from $1 \frac{m^2}{s^2}$ (default value) to $0.1 \frac{m^2}{s^2}$ due to the fact that the backflow air entering the room normal to the pressure outlets is low turbulent air.

Table 1. Calculated temperatures for different part of model (used as boundary conditions for CFD calculations).

Element	Temperature(°C)
Floor	22
Ceiling	24
Large wall	24
Corner	24
Pressure outlets	23
Pipe	24.5
Supplier	27.5

RESULTS AND DISCUSSION

In order to validate the developed model for the temperature field, the temperatures obtained on the simulation and the ones coming from the infrared camera measurement are compared. The first part compared was the flow spreading over the large wall in a zone close to the supply device. Points 1, 2 and 3, in figure 3 left, are chosen for analysis and comparison with the CFD results from figure 4 right (points 1', 2' and 3').

Now, the images taken by infrared camera in the presence of worker will be analysed and compared with the CFD results. We chose an image taken by infrared camera very close to the worker, see figure 4 (left). The analogous plane for this image using the CFD results (figure 4, right) would be a plane crossing the worker at $X = 3$ m.

As can be seen from the both figures, comparing the zone closer to the worker and workbench, both temperature fields have a pretty similar distribution.

Two random areas close to the worker and one more on the upper zone of the room were chosen using ThermaCam Researcher Professional 2.8. The corresponding area and points are chosen for CFD simulation, as in figure 4.

Comparison between points 1, 2 and 3 for both camera image and CFD result is shown in table 3.

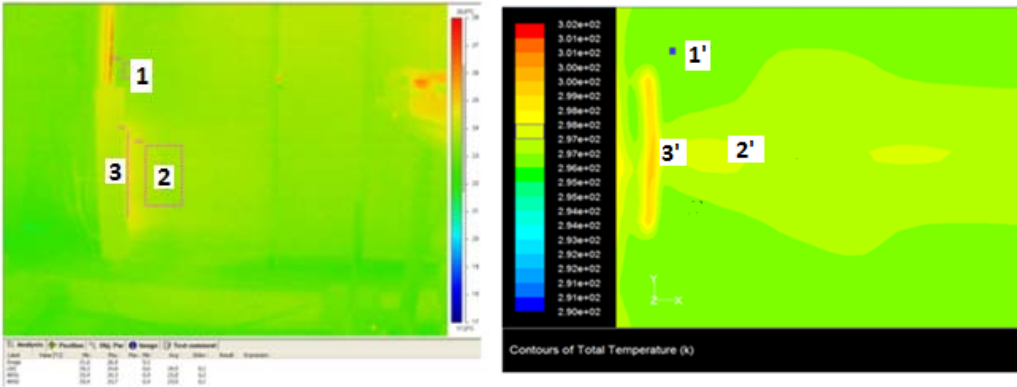


Figure 3. The supplier zone temperature from infrared camera image (left) and Obtained from Fluent (CFD) at z=0.08 is zoomed for deep analysis (right).

Comparing the results in both parts of figure 3 is shown in table 2. As one may observe, the differences are not significant and agree almost well with each other.

Table 2. Temperature difference comparison between CFD results and camera image, figure 3.

	Minimum T [°C]	Maximum T [°C]	Average T [°C]
Object			
1	23.4	23.7	23.5
1'	23	23.6	23.3
Temp. difference	0.4	0.1	0.2
2	23.4	24.3	23.8
2'	23.6	24.2	23.9
Temp. difference	0.2	0.1	0.1
3	24.2	24.8	24.5
3'	24.2	24.8	24.5
Temp. difference	0	0	0

Error was defined as: $error = \frac{(number-number')}{number} * 100$

To be able to analyse and make a proper study of thermal comfort conditions we focus on the near zone (occupied zone) part of the workplace. Two interesting planes at Z = 1m and X = 3m have been chosen for thermal comfort discussions.

For thermal comfort calculations, a worker which releases 2 met while standing and doing a medium effort activity was considered. This metabolic rate, 2 met, is equal to 116 W/m², and it is implemented into Fluent by means of worker boundary conditions, in addition to its corporal temperature, i.e. 37 °C; workbench's temperature is set at 24.5 °C. The operative temperature was checked by using ISO Standard 7730, see Olesen (2002). The clothing consist of briefs, T-shirt, normal trousers, thin sweater, socks, and shoes with gives I_{clu} = 0.04 + 0.09 + 0.25 + 0.2 + 0.02 + 0.02 = 0.62 Clo. The results show that for Clo-value=0.62 and met=2 the operative temperature should be between 23 and 18 °C which is inside the near zone temperature (23 °C).

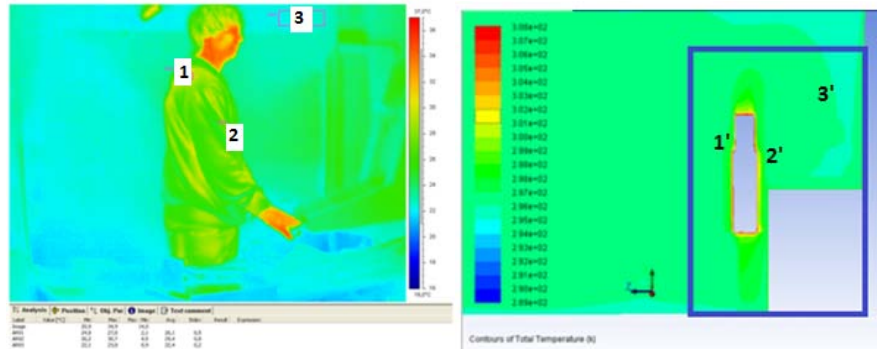


Figure 4. Selected points from infrared camera with worker image (left) and corresponding selected points for temperature field (blue square) nearby the worker at X = 3 m from CFD (right).

Table 3. Worker temperature comparison.

	Minimum T [°C]	Maximum T [°C]	Average T [°C]
Object			
1	26.2	30.7	29.4
1'	28.3	29.2	0.6
Temp. difference	2.1	1.5	- 2.18
2	24.8	27	26.1
2'	25.4	26.4	25.9
Temp. difference	0.6	0.6	0.2
3	22.1	23	22.4
3'	21.7	22.6	22.1
Temp. difference	0.4	0.4	0.3

In order to evaluate the level of dissatisfied with the vertical air temperature difference, the temperature values at neck and ankle level are required. As it is inferred from the following figure 5 (left), the neck temperature is 296 K, while ankle temperature is 295.8 K and hence the temperature difference is 0.2 K. Since every temperature difference below 1 K means 1 % of dissatisfied, a temperature difference of 0.2 results in $PPD = 1 \%$, which is below the upper limit, i.e. 5 %.

As in table 1, the floor temperature is set at 295 K, i.e. 22 °C. By using PPD curve or equation from ISO7730 this floor temperature value gives a predicted percentage of dissatisfied of $PPD = 7 \%$, which is an acceptable value since it is below 10 %, the upper threshold, see Iso7730.

For checking the possible draught problem two methods are carried out here. The first one is to check that velocity at near zone is not higher than 0.15 m/s for heating purposes, while the second uses a formula taking into account mean values for temperature, velocity and turbulence. Therefore these values are to be obtained from Fluent post-processing. The mean temperature that is inferred from vertical air temperature difference study, has a value of 296 K (23 °C). The other data is gathered from the following two figures. It is important to note that the average values obtained may vary due to the calculation complexity, so approximations are presented here.

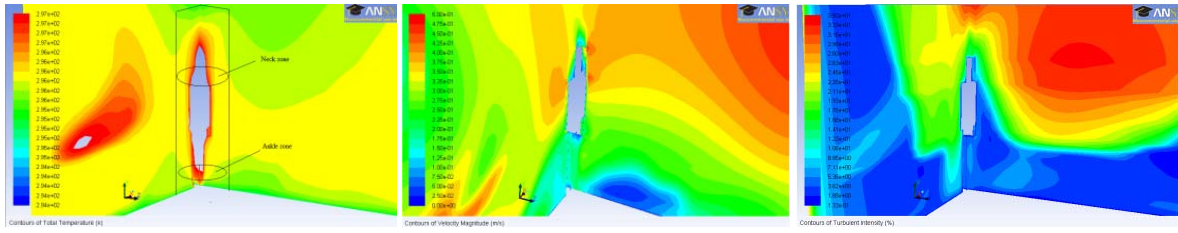


Figure 5. Neck and ankle zone definitions (left), Near zone mean velocity (middle) $U_{\text{mean}} = 0.27 \text{ m/s}$ and near zone mean turbulence intensity (right) $TI_{\text{mean}} = 11.8 \%$ at $Z = 1\text{m}$ and $X = 3\text{m}$.

It has to be pointed out that the first method requirements are not fulfilled since velocity mean value almost doubles the limitation. By means of the second method PD_{draught} (Predicted Dissatisfied due to draught) is calculated as:

$$PD_{\text{draught}} = \left[(34 - T_m) \times (U_m - 0.05)^{0.6223} \right] \times (3.143 + 0.3696 \cdot U_m \times TI_m) =$$

$$[(34 - 23) \times (0.27 - 0.05)^{0.6223}] (3.143 + 0.3696 \times 0.27 \times 11.8) = 18.52 \%$$

The most relevant parts of the human body with regards to draught discomfort are the ankle, the waist and the neck. Therefore, velocity is measured in these places.

$$U_{\text{ankle}} = 0.12 \text{ m/s}; \quad U_{\text{waist}} = 0.18 \text{ m/s}; \quad U_{\text{neck}} = 0.1 \text{ m/s}$$

These values are considered adequate as they fall below maximum recommended velocity (0.15 m/s).

The contours for mean age of air (sec), Predicted Mean Vote (PMV) and Predicted Percentage of Dissatisfied (PPD) are shown in figure 6.

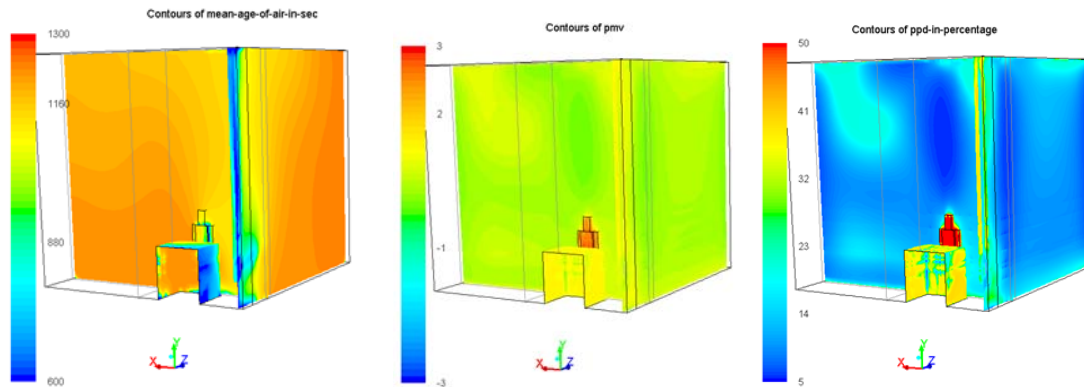


Figure 6. Contours of mean age of air in sec (left), Predicted Mean Vote (PMV, middle) and Predicted Percentage of Dissatisfied (PPV, right) for two cross sections: $x=0.01 \text{ m}$ and $z=1 \text{ m}$.

It is worth mentioning that when developing the model several simplifications were assumed. The real ventilation system consists of 136 air nozzles of 5.6 mm diameter each. This represents a $3.35 \cdot 10^{-3} \text{ m}^2$ area, which has been modelled as a cylindrical section area. It has to be noted that in this investigation, it is assumed that all the airflow is equally distributed between all the nozzles. In addition, the velocity has been set normal to boundary of the air supply area, which is an approximation to reality. Nevertheless, the results obtained represent the expected flow behavior for such a supply terminal.

CONCLUSIONS

This paper focused on infrared camera imaging for temperature mapping and computer simulations of temperature and flow field on an industrial warehouse using a confluent jets air supply.

Concerning thermal comfort, it has to be pointed out that the near zone temperature (23 °C) is within the operative temperature range (18 – 23 °C). Since this value is at the limit of acceptable temperature range, it is recommended that the supply hot air temperature for this building is reduced.

The perceived air quality (PD = 4 %) as well as other indicators, gives PD values below 10 %, which means that ISO 7730 is fulfilled.

From draught analysis it is inferred that values in the occupied zone are slightly higher ($U_{\text{mean}} = 0.27$ m/s) than the recommended value (0.15 m/s). Due to the work activity, higher velocities are considered acceptable while the air velocity in the neck (0.12 m/s), waist (0.18 m/s) and ankle (0.1 m/s) levels are equal or lower than 0.15 m/s. Since velocity at waist level is higher than the acceptable value, it is recommended that the supply outlet velocity is reduced.

It is also pointed out that the higher momentum of Confluent Jets which dominates the thermal buoyancy forces is a major benefit of this system. Observing the velocity and temperature fields, the stratification effects make the system very close to the known displacement ventilation system. Because of limitation of the traditional displacement system for heating (the displacement system is only designed to work for cooling purposes) the confluent jets system can successfully be applied for heating purposes too.

ACKNOWLEDGEMENT

The Swedish Knowledge Foundation (KK.Stiftelsen) is acknowledged for supporting the project. The Authors are also grateful for helps from our students Mr Luis Viguer and Mr Borje Fatas for analyzing our taken images.

REFERENCES

- Awbi HB (2003) *Ventilation of buildings*. London, Spon Press; 2003.
- AIRPAK13.6. User guide. 2007.
- ANSYS 14.5. ANSYS Fluent user guide. 2013.
- Karimipanah T, Awbi H.B., Sandberg M and Blomqvist C (2007) Investigation of air quality, comfort parameters and effectiveness for two floor-level air supply systems in classrooms. *Journal of Building and Environment* 42, Issue 2 (2007) 647-655.
- Bakker A (2002). Applied Computational Fluid Dynamics (Lecture 7- meshing), Fluent inc. (2002).
- Cho Y-J, Awbi H B and Karimipanah T (2008). Theoretical and experimental investigation of wall confluent jets ventilation and comparison with wall displacement ventilation. *Journal of Building and Environment*, 43 (6). pp. 1091-1100. ISSN 0360-1323.
- Cehlin M, Moshfegh B, Sandberg M. (2000) Visualization and Measuring of Air Temperatures Based on Infrared,. *7th International Conference on Air Distribution in Rooms*. Vol1, pp. 339-347.
- Cehlin M, Moshfegh B, Sandberg M. (2002) Measurements of air temperatures close to a low-velocity diffuser in displacement ventilation using an infrared camera. *Energy and Buildings*. 34:687-98.
- FLIR Systems (2006) *ThermaCAMTM Researcher*, Publ. No 1 558 072, Revision a196, Basic Edition, Version 2.8 SR1. Issue date December 21, 2006.
- Lam S H (1992). On the RNG Theory of Turbulence , *Physics of Fluids A*, 4 , pp. 1007-1017, May 1992.
- Olesen BW (2002). Standards for ventilation, IAQ and thermal comfort; 2002.
- Seppänen, O., W.J. Fisk, and Q.H. Lei (2006) Ventilation and performance in office work. *Indoor Air*, 2006. 16(1): p. 28-36.